Time-domain modeling of finite-amplitude sound in relaxing fluids

Robin O. Cleveland,[a] Mark F. Hamilton, and David T. Blackstock
Applied Research Laboratories, The University of Texas at Austin, Austin, Texas 78713-8029 and Department of Mechanical Engineering, The University of Texas at Austin, Austin, Texas 78712-1063

(Received 22 June 1995; accepted for publication 8 February 1996)

A time-domain computer algorithm that solves an augmented Burgers equation is described. The algorithm is a modification of the time-domain code developed by Lee and Hamilton [J. Acoust. Soc. Am. **97**, 906–917 (1995)] for pulsed finite-amplitude sound beams in homogeneous, thermoviscous fluids. In the present paper, effects of nonlinearity, absorption and dispersion (both thermoviscous and relaxational), geometrical spreading, and inhomogeneity of the medium are taken into account. The novel feature of the code is that effects of absorption and dispersion due to multiple relaxation phenomena are included with calculations performed exclusively in the time domain. Numerical results are compared with an analytic solution for a plane step shock in a monorelaxing fluid, and with frequency-domain calculations for a plane harmonic wave in a thermoviscous, monorelaxing fluid. The algorithm is also used to solve an augmented KZK equation that accounts for nonlinearity, thermoviscous absorption, relaxation, and diffraction in directive sound beams. Calculations are presented which demonstrate the effect of relaxation on the propagation of a pulsed, diffracting, finite-amplitude sound beam. © *1996 Acoustical Society of America.*

PACS numbers: 43.25.Cb

INTRODUCTION

A previous article by Lee and Hamilton[1] describes a time-domain algorithm for modeling pulsed finite-amplitude sound beams in homogeneous, thermoviscous fluids. The algorithm accounts for the combined effects of diffraction, absorption, and nonlinearity on the propagation of sound beams radiated by axisymmetric sources. In the same article, a method is proposed for including effects due to multiple relaxation phenomena, each of which introduces dispersion as well as absorption, with time-domain calculations. The main purpose of the present article is to describe implementation of the time-domain relaxation algorithm.

For the case of a finite-amplitude plane wave in a monorelaxing fluid, results from the algorithm are compared with an analytic solution for a step shock, and with numerical solutions obtained with frequency-domain calculations for a waveform that is sinusoidal at the source. Methods for including inhomogeneity of the medium, geometrical spreading, and diffraction in sound beams are also described. Computations for a pulsed finite-amplitude sound beam in a monorelaxing fluid are presented.

Numerical simulations of finite-amplitude propagation in multirelaxing fluids, with geometrical spreading and inhomogeneity taken into account, are reported elsewhere.[2–4] Calculations for the propagation of sonic booms through the atmosphere (modeled as a thermoviscous fluid with two relaxation processes) have revealed that the present time-domain algorithm is more efficient than current frequency-domain algorithms which include the same effects.[5]

[a]Present address: Applied Physics Laboratory, University of Washington, Seattle, WA 98105.

I. NUMERICAL ALGORITHM

We begin with an augmented Burgers equation derived by Pierce,[6] which takes into account the combined effects of nonlinearity, thermoviscous absorption, and an arbitrary number of independent relaxation phenomena on the propagation of progressive plane waves. After combining his Eqs. (11-6.3b) and (11-6.5) we obtain, to the same order of accuracy,

$$\frac{\partial p}{\partial x}=\frac{\beta p}{\rho_0 c_0^3}\frac{\partial p}{\partial t'}+\frac{\delta}{2c_0^3}\frac{\partial^2 p}{\partial t'^2}+\sum_\nu \frac{c_\nu'}{c_0^2}\int_{-\infty}^{t'}\frac{\partial^2 p}{\partial t''^2}\,e^{-(t'-t'')/t_\nu}\,dt''. \tag{1}$$

Here, $p(x,t')$ is sound pressure, x distance, $t'=t-x/c_0$ retarded time, c_0 the equilibrium, small-signal sound speed, ρ_0 the ambient density, β the coefficient of nonlinearity, and δ the diffusivity of sound,[7] due to both viscosity and heat conduction. Each relaxation process ν (where $\nu=1,2,...$) is characterized by a relaxation time t_ν and a small-signal sound-speed increment c_ν'. An alternative form of Eq. (1), in terms of a retarded time based on the frozen sound speed $c_\infty = c_0 + \Sigma_\nu c_\nu'$ instead of the equilibrium sound speed c_0, is given in Appendix A.

Equation (1) is solved in the following dimensionless form:

$$\frac{\partial P}{\partial \sigma}=P\frac{\partial P}{\partial \tau}+\frac{1}{\Gamma}\frac{\partial^2 P}{\partial \tau^2}+\sum_\nu D_\nu\int_{-\infty}^{\tau}\frac{\partial^2 P}{\partial \tau'^2}\,e^{-(\tau-\tau')/\theta_\nu}\,d\tau', \tag{2}$$

where $P(\sigma,\tau)=p/p_0$, p_0 is a reference pressure, $\sigma=x/\overline{x}$,

 0001-4966/96/99(6)/3312/7/$6.00

$\overline{x}=\rho_0 c_0^3/\beta\omega_0 p_0$ is the shock formation distance for a plane wave radiated into an ideal fluid with peak source pressure p_0 and angular frequency ω_0, $\tau=\omega_0 t'$, $\Gamma=1/\alpha_0^{tv}\overline{x}$ is the Gol'dberg number, $\alpha_0^{tv}=\delta\omega_0^2/2c_0^3$ the thermoviscous attenuation coefficient at frequency ω_0, $\theta_\nu=\omega_0 t_\nu$, and $D_\nu = \rho_0 c_0 c_\nu'/\beta p_0$. In terms of these dimensionless quantities, the relaxational attenuation coefficient α_0^{rel} at frequency ω_0 is related to the thermoviscous attenuation coefficient at the same frequency as follows:

$$\frac{\alpha_0^{rel}}{\alpha_0^{tv}}=\Gamma\sum_\nu \frac{D_\nu\theta_\nu}{1+\theta_\nu^2}. \tag{3}$$

Following the methodology used by Lee and Hamilton,[1] we separate Eq. (2) as follows:

$$\frac{\partial P}{\partial\sigma}=P\frac{\partial P}{\partial\tau}, \tag{4}$$

$$\frac{\partial P}{\partial\sigma}=\frac{1}{\Gamma}\frac{\partial^2 P}{\partial\tau^2}, \tag{5}$$

$$\left(\frac{1}{\theta_\nu}+\frac{\partial}{\partial\tau}\right)\frac{\partial P}{\partial\sigma}=D_\nu\frac{\partial^2 P}{\partial\tau^2}, \quad \nu=1,2\ldots . \tag{6}$$

The form of Eq. (6) was obtained by applying the operator $(1/\theta_\nu+\partial/\partial\tau)$ to both sides of Eq. (2) and making use of the relation

$$f(\tau)=\left(\frac{1}{\theta_\nu}+\frac{\partial}{\partial\tau}\right)\int_{-\infty}^{\tau} f(\tau')e^{-(\tau-\tau')/\theta_\nu}\,d\tau'. \tag{7}$$

Equations (4)–(6) are solved independently over each incremental step $\Delta\sigma$. Operator splitting such as this is described in texts on numerical methods.[8,9] Analytic solutions for each of Eqs. (4)–(6) are given in Appendix B, together with verification that in the limit $\Delta\sigma\to 0$, solving Eqs. (4)–(6) independently indeed corresponds to solving Eq. (2). In the algorithm described below, only Eq. (4) is solved analytically. Equations (5) and (6) are solved with finite difference methods.

On the basis of Eq. (B2), Eq. (4) is solved via the time base transformation

$$\tau_i^{k+1}=\tau_i^k-P_i^k\Delta\sigma, \tag{8}$$

where i designates the ith sample of the time waveform and k is the kth step in σ. To ensure that multivalued waveforms are not predicted, the step size restriction on the use of Eq. (8) is

$$\Delta\sigma<\frac{\Delta\tau}{\max\Delta P}, \tag{9}$$

where $\Delta\tau$ is a uniform time sample increment and $\max\Delta P$ is the maximum value of the difference $P_i^k-P_{i-1}^k$ between adjacent pressure samples throughout the entire waveform. Linear interpolation is used to resample the waveform and thus reestablish a uniform time sample spacing $\Delta\tau$ following application of Eq. (8). Lee and Hamilton[1] employed an algorithm that combines the distortion and resampling procedures in a single operation. However, their algorithm can be used only if at each propagation step, Eq. (8) does not advance or delay any time sample by more than $\Delta\tau$. When based on Eq. (8), the step size restriction on their combined algorithm is $\Delta\sigma<\Delta\tau/\max|P|$, which can be much stronger than inequality (9). In the present paper we perform the distortion and resampling procedures independently, and therefore the step size restriction is given by inequality (9).

We use the Crank–Nicolson method to solve Eqs. (5) and (6) with standard forward-space, centered-time finite differences.[8] The finite-difference approximation of each equation is written in the form

$$\mathbf{A}\mathbf{P}^{k+1}=\mathbf{B}\mathbf{P}^k, \tag{10}$$

where the vector $\mathbf{P}^k$ is the uniformly sampled waveform at step k,

$$\mathbf{P}^k=\begin{pmatrix} P_1^k \\ P_2^k \\ \vdots \\ P_{M-1}^k \\ P_M^k \end{pmatrix}, \tag{11}$$

and M is the number of time samples. The tridiagonal matrices $\mathbf{A}$ and $\mathbf{B}$ are given by

$$\mathbf{A}=\begin{pmatrix} 1 & 0 & & & \\ -(r+q) & (1+2r) & -(r-q) & & \\ & \ddots & \ddots & \ddots & \\ & -(r+q) & (1+2r) & -(r-q) & \\ & & 0 & 1 & \end{pmatrix}, \tag{12}$$

$$\mathbf{B}=\begin{pmatrix} 1 & 0 & & & \\ (r-q) & (1-2r) & (r+q) & & \\ & \ddots & \ddots & \ddots & \\ & (r-q) & (1-2r) & (r+q) & \\ & & 0 & 1 & \end{pmatrix}, \tag{13}$$

where $r=\Delta\sigma/2\Gamma(\Delta\tau)^2$ and $q=0$ for Eq. (5), $r=D_\nu\theta_\nu\Delta\sigma/2(\Delta\tau)^2$ and $q=\theta_\nu/2\Delta\tau$ for Eq. (6), and we have imposed the boundary conditions $P_1^{k+1}=P_1^k$ and $P_M^{k+1}=P_M^k$ at the ends of the time window. The solution vector $\mathbf{P}^{k+1}$ is calculated explicitly in order M operations with the Thomas algorithm.[8]

Because of resampling, a statement made by Lee and Hamilton[1] that thermoviscous absorption predicted Eq. (5) is underestimated by Eq. (10) warrants clarification. Although the statement is true (see Ref. 10 for further discussion with numerical results), it was found that the effect of resampling the waveform after the time base distortion in Eq. (8) is applied introduces numerical absorption that can more than compensate for the underestimation of absorption by the finite-difference approximation.

We also call attention to a potential problem with the relaxation algorithm in the limit $\Delta\sigma\to 0$. Normally, the time sample spacing $\Delta\tau$ is much less than the relaxation time θ_ν, and $q\gg 1$ is obtained. For $\Delta\sigma$ sufficiently small we also have $q\gg r$, and the off-diagonal elements in both $\mathbf{A}$ and $\mathbf{B}$ then dominate the diagonal elements. The matrices are ill-conditioned in this case, and large numerical errors can re-

sult. The errors can be reduced by giving greater weighting to the backward difference in the Crank–Nicolson scheme.[8] However, we have encountered this source of error only for exceedingly small values of $\Delta\sigma$, not for values typically required to accurately model common physical situations. A similar problem does not arise with the absorption algorithm in the limit $\Delta\sigma\rightarrow 0$, because $q=0$.

Equations (4)–(6) are solved sequentially over each step. Given a waveform at step k, Eq. (5) is solved via Eq. (10) to include the effect of thermoviscous absorption on the wave as it propagates to step $k+1$. The resulting solution at step $k+1$ becomes the input back at step k for the solution of Eq. (10) corresponding to the first of Eqs. (6). The solution at step $k+1$ now includes the effects of thermoviscous absorption and one relaxation process. The same procedure is repeated for all remaining relaxation equations. Finally, the result from the last relaxation equation becomes the input back at step k for the nonlinearity algorithm, Eq. (8), based on Eq. (4). The output from the nonlinearity algorithm thus approximates the solution of Eq. (2) over a single incremental step $\Delta\sigma$ (see the last paragraph in Appendix B). The waveform is resampled, and the algorithm is repeated over all subsequent steps. An analysis of the cumulative numerical error in a similar algorithm that solves the KZK equation is provided by the discussion of Fig. 2 in Ref. 1.

II. BENCHMARK TESTS

To test the relaxation algorithm, we first compare numerical results with an analytic solution derived by Polyakova *et al.*[11] for a monorelaxing fluid. Their solution applies to a stationary wave, for which $\partial P/\partial\sigma=0$ in the retarded time frame, with a pressure jump defined by $P=1$ at $\tau=\infty$ and $P=-1$ at $\tau=-\infty$ (the net overpressure is thus $2p_0$). In the absence of thermoviscous absorption ($\Gamma=\infty$) and with only one relaxation term retained in Eq. (2), they derived the exact solution

$$\tau=\theta\,\ln\frac{(1+P)^{D-1}}{(1-P)^{D+1}}, \tag{14}$$

where the subscripts on D and θ have been suppressed. The constant of integration in Eq. (14) was chosen such that $P=0$ at $\tau=0$.

For $D<1$, nonlinearity is sufficiently strong that Eq. (14) describes a multivalued waveform. Weak shock theory can be used to correct the solution, which yields (see Pierce,[6] p. 592)

$$P_s=1-2D, \quad 0\leqslant D\leqslant 1, \tag{15}$$

for the peak shock pressure. The shock pressure thus increases linearly from $P_s=-1$ to $P_s=1$ as D decreases from 1 (the shock threshold) to 0 (no dispersion). The arrival time τ_s of the shock is determined by setting $P=P_s$ in Eq. (14):

$$\tau_s=-\theta\,\ln[4D^{1+D}(1-D)^{1-D}], \quad 0\leqslant D\leqslant 1. \tag{16}$$

To construct the wave profile for $0\leqslant D\leqslant 1$, set $P=-1$ for $\tau<\tau_s$ and

$$\tau=\tau_s, \quad -1\leqslant P\leqslant P_s, \tag{17}$$

$$=\theta\,\ln\frac{(1+P)^{D-1}}{(1-P)^{D+1}}, \quad P_s\leqslant P\leqslant 1. \tag{18}$$

Equation (14) is plotted in Fig. 1(a) (dashed line) for $D=0.5$. The solid line is the corrected, single-valued solution obtained using Eqs. (15)–(18), which for this case yield $P_s=0$ and $\tau_s=0$.

We now demonstrate that the numerical algorithm converges to the solid line in Fig. 1(a) for σ sufficiently large. Since losses introduced by relaxation are insufficient to stabilize shock formation, thermoviscous losses must be retained in the algorithm. The thermoviscous losses are kept sufficiently small that their main effect is to control the rise time of the shock without significantly affecting other portions of the wave. Numerical solutions of Eq. (2) were obtained with $D=0.5$, $\theta=1/6$, and $\Gamma=2000$. The input waveform at $\sigma=0$, shown as a dashed line in Fig. 1(b), is a step shock described by 8192 uniformly spaced points in the domain $-3\pi\leqslant\tau/\theta\leqslant 9\pi$. Calculations were performed with $\Delta\sigma=1.2\times10^{-3}$. At $\sigma=5$ the waveform attained the stationary profile shown as the solid line in Fig. 1(b). In Fig. 1(c), the analytic solution [dashed line, repeated from Fig. 1(a)] is compared with the numerical result [solid line, repeated from Fig. 1(b) but translated slightly in time to line up with the analytic solution]. Agreement between the numerical and analytic solutions is very good.

Time-domain calculations were also compared with results corresponding to a case considered by Hamilton *et al.*,[12] who report computations performed in the frequency domain for a harmonic wave in a monorelaxing, thermoviscous fluid. The source waveform is sinusoidal, with $D=0.5$, $\theta=1$, and $\Gamma=400$ (for which $\alpha_0^{rel}/\alpha_0^{tv}=100$). To simulate a periodic waveform, the time-domain calculations were performed for a three-cycle tone burst, and results are presented only for the middle cycle. We used 1600 samples per cycle for the time-domain calculations, 800 harmonics for the frequency-domain calculations (see Ref. 12 for discussion of the frequency-domain algorithm), and $\Delta\sigma=10^{-3}$ for both cases. Results for several values of σ are shown in Fig. 2, where the solid lines for the time-domain calculations and the dashed lines for the frequency-domain calculations are virtually indistinguishable.

Although the calculations in Figs. 1 and 2 pertain to a monorelaxing fluid, no additional difficulties are encountered when more than one relaxation process is included. Results presented elsewhere,[2,4] for sonic boom shock profiles with two relaxation processes (oxygen and nitrogen) as well as thermoviscous losses taken into account, are in excellent agreement with results from other methods of calculation.

III. OTHER EFFECTS

Here we describe methods for including effects due to geometrical spreading, inhomogeneity, and diffraction. We first describe a method for solving an augmented Burgers equation that takes geometrical spreading and inhomogeneity into account. Numerical results obtained using this equation to model sonic boom propagation through a stratified atmo-

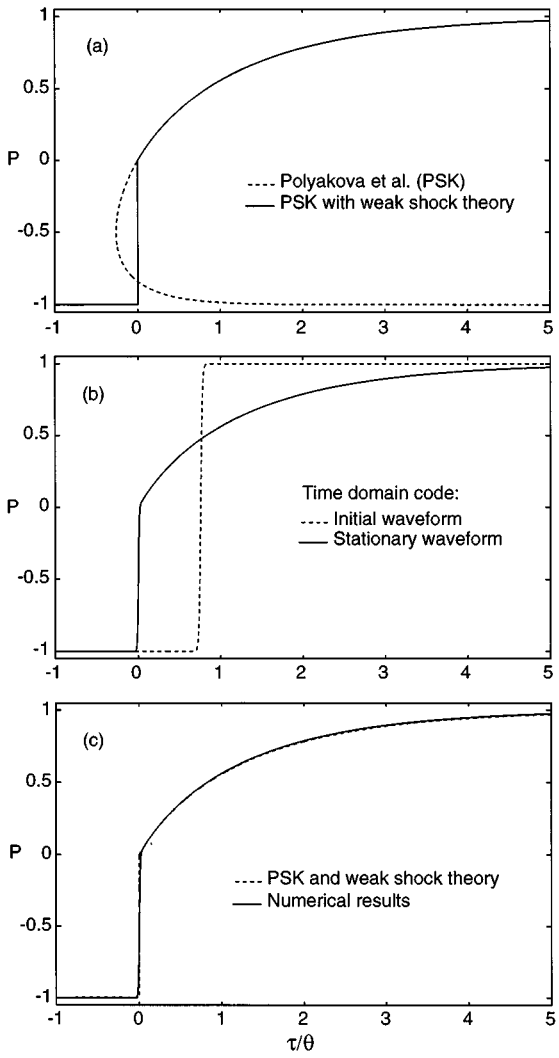

FIG. 1. Comparison of steady-state numerical result with analytic solution derived by Polyakova *et al.*[11] for a plane step shock in a monorelaxing fluid. (a) Multivalued analytic solution (dashed line), and correction based on weak shock theory (solid line). (b) Initial waveform for numerical algorithm (dashed line), and calculated steady-state waveform (solid line). (c) Comparison of numerical result (solid line) with analytic solution (dashed line).

sphere have been reported elsewhere.[3,4] Second, we present calculations, based on an augmented KZK equation, demonstrating the combined effects of nonlinearity, diffraction, thermoviscous absorption, and relaxation on a pulsed sound beam in a homogeneous fluid.

A. Geometrical spreading and inhomogeneous media

Equation (1) can be augmented to include geometrical spreading and inhomogeneity. It is assumed that the spreading and the local values of the ambient fluid properties vary slowly on the scale of a wavelength (i.e., $L \gg \lambda$, where L characterizes the length scale corresponding to variations in the spreading or inhomogeneity, and λ is the characteristic wavelength). In the geometrical acoustics approximation, the augmented form of Eq. (1) becomes (see, e.g., Morfey and Cotaras[13])

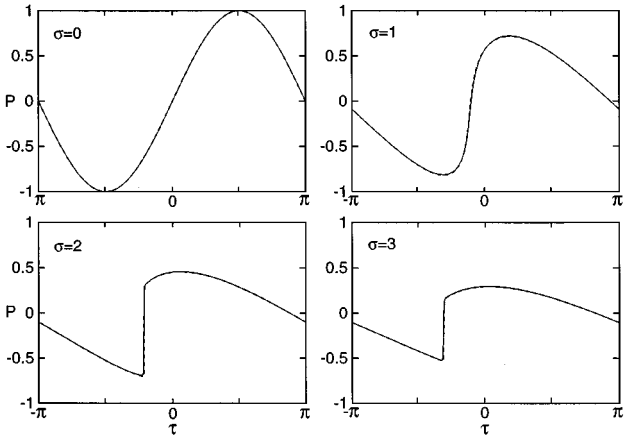

FIG. 2. Comparison of time-domain calculations (solid lines) with frequency-domain calculations (dashed lines) for an initially sinusoidal plane wave in a monorelaxing, thermoviscous fluid.

$$\frac{\partial p}{\partial s} + \left(\frac{d}{ds} \ln \sqrt{\frac{A}{\rho_0 c_0}} \right) p = \frac{\beta p}{\rho_0 c_0^3} \frac{\partial p}{\partial t'} + \frac{\delta}{2 c_0^3} \frac{\partial^2 p}{\partial t'^2} + \sum_\nu \frac{c'_\nu}{c_0^2} \int_{-\infty}^{t'} \frac{\partial^2 p}{\partial t''^2} e^{-(t'-t'')/t_\nu} \, dt'', \tag{19}$$

where propagation is along a ray tube with area $A(s)$, s is distance from the source along the ray path, all ambient fluid properties $(\rho_0, c_0, \beta, \delta, c'_\nu, t_\nu)$ may vary with s, and the retarded time is given here by $t' = t - \int_0^s ds'/c_0(s')$.

The dimensionless notation used below is based on the ambient properties at $s=0$, i.e., $\sigma = s/\overline{x}$, where the plane wave shock formation distance $\overline{x}$, as well as Γ, θ_ν, and D_ν, are constants defined as before and evaluated at $\sigma=0$. Let $\tau = \omega_0 t'$, and to eliminate the second term on the left-hand side of Eq. (19) let $P = (S/Z)^{1/2} p/p_0$, where $S(\sigma) = A(\sigma)/A(0)$ and $Z(\sigma) = \rho_0(\sigma) c_0(\sigma)/\rho_0(0) c_0(0)$. Equation (19) thus reduces to

$$\frac{\partial P}{\partial \sigma} = \Phi^{nl} P \frac{\partial P}{\partial \tau} + \frac{\Phi^{tv}}{\Gamma} \frac{\partial^2 P}{\partial \tau^2} + \sum_\nu D_\nu \Phi_\nu^{rc} \int_{-\infty}^{\tau} \frac{\partial^2 P}{\partial \tau'^2} e^{-(\tau-\tau')\Phi_\nu^{rt}/\theta_\nu} \, d\tau', \tag{20}$$

where the effects of inhomogeneity are taken into account by the functions $\Phi(\sigma)$: $\Phi^{nl}(\sigma) = [\Lambda(\sigma)/\Lambda(0)]/\sqrt{S(\sigma)}$, where expressions for $\Lambda = \beta/(\rho_0 c_0^5)^{1/2}$ for fresh water and seawater are presented by Cotaras and Morfey;[14] $\Phi^{tv}(\sigma) = \alpha_0^{tv}(\sigma)/\alpha_0^{tv}(0)$ defines the variation in thermoviscous attenuation; $\Phi_\nu^{rc}(\sigma) = [c'_\nu(\sigma)/c'_\nu(0)]/[c_0(\sigma)/c_0(0)]^2$ and $\Phi_\nu^{rt}(\sigma) = t_\nu(0)/t_\nu(\sigma)$ account for variations in the relaxation processes. At the source, or for a homogeneous fluid and with no geometrical spreading, $\Phi=1$ and Eq. (20) reduces to Eq. (2).

Now separate Eq. (20) as follows:

$$\frac{\partial P}{\partial \sigma} = \Phi^{nl} P \frac{\partial P}{\partial \tau}, \tag{21}$$

$$\frac{\partial P}{\partial \sigma} = \frac{\Phi^{tv}}{\Gamma} \frac{\partial^2 P}{\partial \tau^2}, \tag{22}$$

$$\left(\frac{\Phi_\nu^{rt}}{\theta_\nu} + \frac{\partial}{\partial \tau} \right) \frac{\partial P}{\partial \sigma} = D_\nu \Phi_\nu^{rc} \frac{\partial^2 P}{\partial \tau^2}, \quad \nu = 1,2,\ldots . \tag{23}$$

Equations (21)–(23) are solved in essentially the same way as Eqs. (4)–(6). In Eq. (8) replace P_i^k by $\Phi_k^{nl} P_i^k$, and in the expressions for r and q in Eqs. (12) and (13) replace Γ by Γ/Φ_k^{tv}, D_ν by $D_\nu \Phi_{\nu,k}^{rc}$, and θ_ν by $\theta_\nu/\Phi_{\nu,k}^{rt}$, where Φ_k is the value of $\Phi(\sigma)$ at step k. A separate algorithm may be required to determine the ray path (see, for example, Anderson *et al.*[15] or Foreman[16]) in order to specify the ambient fluid properties and ray tube area as functions of σ. To within the accuracy of the approximations used to derive Eq. (19), it is consistent to employ small-signal theory to calculate the ray paths.[13]

For a homogeneous fluid but with geometrical spreading taken into account, the relations $\Phi^{nl} = S^{-1/2}$ and $\Phi^{tv} = \Phi_\nu^{rt} = \Phi_\nu^{rc} = Z = 1$ are obtained. If the spreading is cylindrical ($m = 1/2$) or spherical ($m = 1$), then $S = (1 + \sigma/\sigma_0)^{2m}$, where $\sigma_0 = r_0/\overline{x}$, and r_0 is the radius of the source.

B. Diffraction in sound beams

A time-domain algorithm for modeling the combined effects of diffraction, thermoviscous absorption, and nonlinearity on directive, axisymmetric sound beams in homogeneous fluids was reported previously.[1] When axisymmetric beam diffraction is included, Eq. (1) becomes the following augmented KZK equation in cylindrical coordinates:

$$\frac{\partial p}{\partial x} = \frac{c_0}{2} \int_{-\infty}^{t'} \left(\frac{\partial^2 p}{\partial r^2} + \frac{1}{r} \frac{\partial p}{\partial r} \right) dt'' + \frac{\beta p}{\rho_0 c_0^3} \frac{\partial p}{\partial t'} + \frac{\delta}{2 c_0^3} \frac{\partial^2 p}{\partial t'^2} + \sum_\nu \frac{c_\nu'}{c_0^2} \int_{-\infty}^{t'} \frac{\partial^2 p}{\partial t''^2} e^{-(t'-t'')/t_\nu} \, dt'', \tag{24}$$

where x is the coordinate along the axis of the beam, $t' = t - x/c_0$ is the retarded time used in Sec. I, and r is distance from the axis. Effects of diffraction and nonlinearity are computed with the algorithm described in Ref. 1, with thermoviscous absorption and relaxation taken into account as described in Sec. I above.

Numerical results are presented in Fig. 3 for a short tone burst radiated by a circular piston of radius a in a thermoviscous, monorelaxing fluid. We introduce the Rayleigh distance $x_0 = \omega_0 a^2/2c_0$ and relate the parameters used in the previous article[1] to those employed here as follows: $N = x_0/\overline{x}$, $A = N/\Gamma$, $C_\nu = N D_\nu \theta_\nu$. The calculations were performed with $N = 1$, $A = 0.01$, $\theta = 1$, and $C = 1$ (for which $\Gamma = 100$, $D = 1$, $\alpha_0^{rel}/\alpha_0^{tv} = 50$), and with the following source waveform prescribed on the surface of the piston:

$$P = \exp[-(\tau/3\pi)^8] \sin \tau, \quad \sigma = 0. \tag{25}$$

The solid lines for $\sigma > 0$ in Fig. 3 are the waveforms calculated along the axis of the beam, and the dashed lines are the corresponding results obtained when effects of relaxation were not included. Since $N = 1$ in the present example, we have $\sigma = x/\overline{x} = x/x_0$. At $\sigma = 1$, relaxation advances the pulse in time and reduces the peak-to-peak amplitude by approximately 50%. Although the rise times of the shocks are slightly increased, the overall wave profile is similar to the case without relaxation. Relaxation introduces substantial rounding of the wave profiles following the shocks at $\sigma = 2$, as in Fig. 2. At $\sigma = 4$, relaxation causes the waveforms to have rounded positive portions and cusped negative portions, in contrast to the sharp peaks and elongated troughs that result from the combined effects of diffraction and nonlinearity in the absence of relaxation.

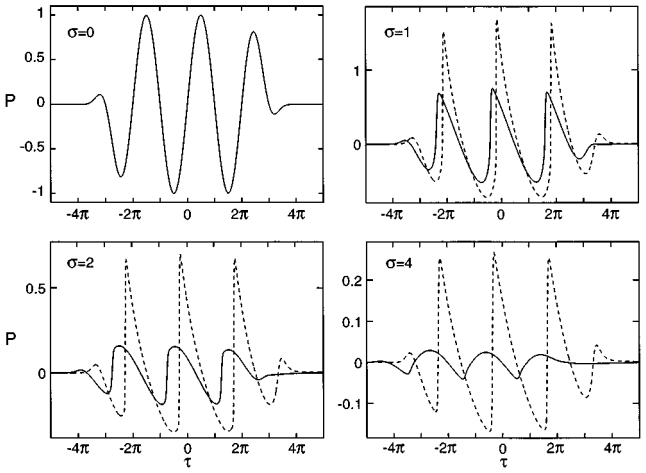

FIG. 3. Numerical results for waveforms along the axis of a pulsed finite-amplitude sound beam radiated by a circular piston in a monorelaxing, thermoviscous fluid (solid lines), compared with corresponding numerical results without relaxation taken into account (dashed lines).

IV. SUMMARY

A time-domain algorithm that includes the effects of relaxation on the propagation of finite-amplitude sound was described. Results obtained from the algorithm were compared with an analytic solution for a step shock, and with frequency-domain calculations for a time-harmonic wave. Methods for taking thermoviscous absorption, geometrical spreading, and inhomogeneity of the medium into account were also described. Numerical results were presented for diffraction of a pulsed finite-amplitude sound beam in a relaxing fluid.

ACKNOWLEDGMENTS

Discussions with Yu. A. Il'inskii, O. A. Sapozhnikov, and D. E. Wilson are gratefully acknowledged. This work was supported by the National Aeronautics and Space Administration, the Office of Naval Research, and the Internal Research and Development Program at Applied Research Laboratories. All computations were performed on IBM RISC 6000 workstations in the Department of Mechanical Engineering.

APPENDIX A: ALTERNATIVE FORM OF EQ. (1)

Here we rewrite Eq. (1) in terms of a retarded time based on the frozen sound speed $c_\infty = c_0 + \Sigma_\nu c'_\nu$ rather than the equilibrium sound speed c_0. Begin by integrating the relaxation term in Eq. (1) by parts to obtain

$$\frac{\partial p}{\partial x} = \frac{\beta p}{\rho_0 c_0^3}\frac{\partial p}{\partial t'} + \frac{\delta}{2c_0^3}\frac{\partial^2 p}{\partial t'^2} + \left(\sum_\nu c'_\nu\right)\frac{1}{c_0^2}\frac{\partial p}{\partial t'} - \sum_\nu \frac{c'_\nu}{c_0^2 t_\nu}\int_{-\infty}^{t'}\frac{\partial p}{\partial t''}\, e^{-(t'-t'')/t_\nu}\, dt'', \tag{A1}$$

where $t' = t - x/c_0$. Now let $t'_\infty = t - x/c_\infty$, which after expansion up to lowest order in the small quantities c'_ν differs from t' according to the relation

$$t'_\infty = t' + \frac{x}{c_0^2}\sum_\nu c'_\nu. \tag{A2}$$

Use of Eq. (A2) to transform Eq. (A1) from the coordinate system (x,t') to (x,t'_∞) yields

$$\frac{\partial p}{\partial x} = \frac{\beta p}{\rho_0 c_0^3}\frac{\partial p}{\partial t'_\infty} + \frac{\delta}{2c_0^3}\frac{\partial^2 p}{\partial t'^2_\infty} - \sum_\nu \frac{c'_\nu}{c_0^2 t_\nu}\int_{-\infty}^{t'_\infty}\frac{\partial p}{\partial t''}\, e^{-(t'_\infty - t'')/t_\nu}\, dt''. \tag{A3}$$

In terms of the dimensionless quantities defined following Eq. (2), Eq. (A3) becomes

$$\frac{\partial P}{\partial \sigma} = P\frac{\partial P}{\partial \tau_\infty} + \frac{1}{\Gamma}\frac{\partial^2 P}{\partial \tau_\infty^2} - \sum_\nu \frac{D_\nu}{\theta_\nu}\int_{-\infty}^{\tau_\infty}\frac{\partial P}{\partial \tau'}\, e^{-(\tau_\infty - \tau')/\theta_\nu}\, d\tau', \tag{A4}$$

where $\tau_\infty = \omega_0 t'_\infty$. To within the order of accuracy of the augmented Burgers equation, c_0 may be replaced by c_∞ in the expressions for Γ and D_ν, i.e., in the coefficients on the right-hand side of Eq. (A3). The formalism of the algorithm described in Sec. I remains the same, but with τ replaced by τ_∞ in Eqs. (4) and (5), and with Eq. (6) replaced by

$$\left(1 + \theta_\nu \frac{\partial}{\partial \tau_\infty}\right)\frac{\partial P}{\partial \sigma} = -D_\nu \frac{\partial P}{\partial \tau_\infty}, \quad \nu = 1,2,\ldots . \tag{A5}$$

For numerical stability, backward time differences must be used to approximate Eq. (A5), in which case different forms of Eqs. (12) and (13) are obtained.[8]

APPENDIX B: ANALYTIC SOLUTIONS OF EQS. (4)–(6)

Presented below are analytic expressions, obtained from each of Eqs. (4)–(6) individually, for the waveform at $\sigma+\Delta\sigma$ in terms of the waveform at σ. We also demonstrate that in the limit $\Delta\sigma \to 0$, solving Eqs. (4)–(6) independently as described in Sec. I indeed corresponds to solving Eq. (2).

Equation (4) is satisfied by the Poisson solution

$$P(\sigma,\tau) = F(\tau + \sigma P), \tag{B1}$$

where $F(\tau)$ is the waveform at the source. To describe propagation of the waveform from σ to $\sigma+\Delta\sigma$, the Poisson solution may be rewritten

$$P(\sigma+\Delta\sigma,\tau) = P(\sigma,\tau+P\Delta\sigma). \tag{B2}$$

Multivalued solutions are avoided if the inequality

$$\Delta\sigma < \frac{1}{\max(\partial P/\partial\tau)} \tag{B3}$$

is satisfied. Expansion of Eq. (B2) to first order in $\Delta\sigma$ yields Eq. (4) in the limit $\Delta\sigma \to 0$.

Equation (5) is the diffusion equation, and its solution is given by

$$P(\sigma+\Delta\sigma,\tau) = \int_{-\infty}^{\infty} P(\sigma,\tau')H_{tv}(\Delta\sigma,\tau-\tau')\,d\tau', \tag{B4}$$

where the impulse response is defined by[7]

$$H_{tv}(\sigma,\tau) = \sqrt{\Gamma/4\pi\sigma}\,\exp(-\Gamma\tau^2/4\sigma). \tag{B5}$$

Equation (B5) can be rewritten as the following Taylor series expansion:

$$H_{tv}(\Delta\sigma,\tau) = \sum_{n=0}^{\infty}\frac{1}{n!}\left(\frac{\Delta\sigma}{\Gamma}\right)^n \delta^{(2n)}(\tau), \tag{B6}$$

where $\delta(\tau)$ is the Dirac delta function, and $\delta^{(n)}(\tau)$ is its nth derivative with respect to τ. Substitution of Eq. (B6) into Eq. (B4) yields Eq. (5) in the limit $\Delta\sigma \to 0$.

The solution of Eq. (6) is

$$P(\sigma+\Delta\sigma,\tau) = \int_{-\infty}^{\infty} P(\sigma,\tau')H_{rel}(\Delta\sigma,\tau-\tau')\,d\tau'. \tag{B7}$$

The natural coordinate system for the impulse response of a relaxing fluid is in a retarded time frame based on the frozen sound speed. We therefore start with the impulse response of Eq. (A5), with the subscript ν suppressed:[17]

$$H_{rel}(\sigma,\tau_\infty) = \exp\left(-\frac{D\sigma}{\theta}\right)\left\{\delta(\tau_\infty) + \left(\frac{D\sigma}{\theta^2}\right)e^{-\tau_\infty/\theta}u(\tau_\infty)\,\frac{I_1[2(D\sigma\tau_\infty/\theta^2)^{1/2}]}{(D\sigma\tau_\infty/\theta^2)^{1/2}}\right\}, \tag{B8}$$

where I_1 is the modified Bessel function of the first kind, of order one, and u is the unit step function, i.e., $u(\tau)=0$ for $\tau<0$ and $u(\tau)=1$ for $\tau>0$. To obtain the impulse response of Eq. (6), substitute the relation $\tau_\infty = \tau + D\sigma$ from Eq. (A2) into Eq. (B8). In the retarded time frame τ, the Taylor series expansion of H_{rel} through terms of order $\Delta\sigma$ is

$$H_{rel}(\Delta\sigma,\tau) = \delta(\tau) + D\Delta\sigma[\delta^{(1)}(\tau) - \theta^{-1}\delta(\tau) + \theta^{-2}e^{-\tau/\theta}u(\tau)] + O[(\Delta\sigma)^2]. \tag{B9}$$

Substitution of Eq. (B9) into Eq. (B7) yields, in the limit $\Delta\sigma \to 0$,

$$\frac{\partial P}{\partial \sigma} = D\left(\frac{\partial P}{\partial \tau} - \frac{1}{\theta}P + \frac{1}{\theta^2}\int_{-\infty}^{\tau} P(\sigma,\tau')e^{-(\tau-\tau')/\theta}\,d\tau'\right). \tag{B10}$$

Equation (B10) is equivalent to Eq. (6), obtained by integrating the relaxation term in Eq. (2) twice by parts for the case of a single process.

Finally, we make some remarks about operator splitting. In Sec. I we described an algorithm for solving Eq. (2) numerically using a splitting procedure in which various components of the equation, namely Eqs. (4)–(6), are solved separately. Although the splitting method (also referred to as the method of fractional steps) is well documented,[8,9] a specific verification that our algorithm does indeed correspond to solving Eq. (2) in the limit $\Delta\sigma\rightarrow 0$ may be of interest. Let $\tilde{H}_{tv}$ and $\tilde{H}_{rel}$ be the Taylor series expansions of H_{tv} and H_{rel}, respectively, through terms of order $\Delta\sigma$. From Eq. (B6) we thus have

$$\tilde{H}_{tv}(\Delta\sigma,\tau)=\delta(\tau)+(\Delta\sigma/\Gamma)\,\delta^{(2)}(\tau)+O[(\Delta\sigma)^2],$$

with $\tilde{H}_{rel}(\Delta\sigma,\tau)$ given by Eq. (B9). Given a waveform $P(\sigma,\tau)$ at step σ, let $P_1(\sigma+\Delta\sigma,\tau)$ designate the solution at step $\sigma+\Delta\sigma$ due to solving Eq. (5):

$$P_1(\sigma+\Delta\sigma,\tau)=\int_{-\infty}^{\infty}P(\sigma,\tau')\tilde{H}_{tv}(\Delta\sigma,\tau-\tau')\,d\tau'+O[(\Delta\sigma)^2]. \tag{B11}$$

We next include the effect of one relaxation process by taking the solution $P_1(\sigma+\Delta\sigma,\tau)$ to be the input back at step σ and letting $P_2(\sigma+\Delta\sigma,\tau)$ designate the resulting solution of Eq. (6):

$$P_2(\sigma+\Delta\sigma,\tau)=\int_{-\infty}^{\infty}P_1(\sigma+\Delta\sigma,\tau')\tilde{H}_{rel}(\Delta\sigma,\tau-\tau')\,d\tau'+O[(\Delta\sigma)^2]. \tag{B12}$$

Nonlinearity is included by taking $P_2(\sigma+\Delta\sigma,\tau)$ to be the input back at step σ for the solution of Eq. (4). This final solution, which we designate $P(\sigma+\Delta\sigma,\tau)$, is obtained by expanding Eq. (B2) to obtain

$$P(\sigma+\Delta\sigma,\tau)=P_2(\sigma+\Delta\sigma,\tau)+P_2\,\frac{\partial P_2}{\partial\tau}\,\Delta\sigma+O[(\Delta\sigma)^2]. \tag{B13}$$

Combining Eqs. (B11)–(B13) after performing the integrations yields

$$P(\sigma+\Delta\sigma,\tau)=P(\sigma,\tau)+\Delta\sigma\left[P\,\frac{\partial P}{\partial\tau}+\frac{1}{\Gamma}\,\frac{\partial^2 P}{\partial\tau^2}+D\left(\frac{\partial P}{\partial\tau}-\frac{1}{\theta}\,P+\frac{1}{\theta^2}\int_{-\infty}^{\tau}P(\sigma,\tau')e^{-(\tau-\tau')/\theta}d\tau'\right)\right]+O[(\Delta\sigma)^2], \tag{B14}$$

which in the limit $\Delta\sigma\rightarrow 0$ reduces to Eq. (2) for the case of a single relaxation process [with the remark following Eq. (B10) taken into consideration].

[1] Y.-S. Lee and M. F. Hamilton, ''Time-domain modeling of pulsed finite-amplitude sound beams,'' J. Acoust. Soc. Am. **97**, 906–917 (1995).

[2] R. O. Cleveland, M. F. Hamilton, and D. T. Blackstock, ''Effect of stratification of the atmosphere on sonic boom propagation,'' in *Proceedings of the Sixth International Symposium on Long-Range Sound Propagation*, compiled by D. I. Havelock and M. R. Stinson (National Research Council, Ottawa, 1994), pp. 59–76. Note that the third term in Eq. (4) contains a sign error.

[3] R. O. Cleveland, ''Propagation of sonic booms through a real, stratified atmosphere,'' Ph.D. dissertation, The University of Texas at Austin (1995).

[4] R. O. Cleveland, M. F. Hamilton, and D. T. Blackstock, ''THOR: A time domain algorithm for propagation of sonic booms and other finite-amplitude waves in real, inhomogeneous fluids,'' *Proceedings of the 15th International Congress on Acoustics*, edited by M. Newman (Trondheim, Norway, June 1995), Vol. IV, pp. 393–396.

[5] J. P. Chambers, H. E. Bass, R. Raspet, R. O. Cleveland, M. F. Hamilton, and D. T. Blackstock, ''Comparison of computer codes for propagation of sonic booms through the atmosphere,'' J. Acoust. Soc. Am. **97**, 3259(A) (1995).

[6] A. D. Pierce, *Acoustics—An Introduction to Its Physical Principles and Applications* (Acoustical Society of America, New York, 1989).

[7] J. Lighthill, *Waves in Fluids* (Cambridge U.P., Cambridge, 1980), Sec. 1.13.

[8] W. F. Ames, *Numerical Methods for Partial Differential Equations* (Academic, New York, 1992), 3rd ed.

[9] W. H. Press, S. A. Teukolsky, W. T. Vetterling, and B. P. Flannery, *Numerical Recipes in FORTRAN* (Cambridge U.P., New York, 1992), 2nd ed., pp. 847–848.

[10] M. F. Hamilton, Yu. A. Il'insky, and E. A. Zabolotskaya, ''Evolution equations for nonlinear Rayleigh waves,'' J. Acoust. Soc. Am. **97**, 891–897 (1995).

[11] A. L. Polyakova, S. I. Soluyan, and R. V. Khokhlov, ''Propagation of finite disturbances in a relaxing medium,'' Sov. Phys. Acoust. **8**, 78–82 (1962).

[12] M. F. Hamilton, Yu. A. Il'inskii, and E. A. Zabolotskaya, ''Dispersion,'' to appear in *Nonlinear Acoustics*, edited by D. T. Blackstock and M. F. Hamilton (Academic, New York, 1997), Chap. 5.

[13] C. L. Morfey and F. D. Cotaras, ''Propagation in inhomogeneous media (ray theory),'' to appear in *Nonlinear Acoustics*, edited by D. T. Blackstock and M. F. Hamilton (Academic, New York, 1997), Chap. 12.

[14] F. D. Cotaras and C. L. Morfey, ''Polynomial expressions for the coefficient of nonlinearity β and $\beta/(\rho c^5)^{1/2}$ for fresh water and seawater,'' J. Acoust. Soc. Am. **94**, 585–588 (1993).

[15] G. Anderson, R. Gocht, and D. Sirota, ''Spreading loss of sound in an inhomogeneous medium,'' J. Acoust. Soc. Am. **36**, 140–145 (1964).

[16] T. L. Foreman, ''Ray modeling methods for range dependent ocean environments,'' Tech. Rep. ARL-TR-83-41, Applied Research Laboratories, The University of Texas at Austin (1983).

[17] V. G. Andreev, O. A. Sapozhnikov, and S. T. Timofeev, ''Evolution of pulses in a relaxational medium,'' Acoust. Phys. **40**, 172–175 (1994).